Eur Biophys J (1999) 28: 187–199

ARTICLE

Albert J. Jin · Daniel Huster · Klaus Gawrisch
Ralph Nossal

Light scattering characterization of extruded lipid vesicles

Received: 31 July 1998 / Revised version: 26 October 1998 / Accepted: 5 November 1998

Abstract By modeling extruded unilamellar lipid vesicles as thin-walled ellipsoidal shells, mathematical analysis provides simple equations which relate the mean elongation and other morphological characteristics of a vesicle population to quantities readily obtained from combined static and dynamic light scattering measurements. For SOPC vesicles extruded through a 100 nm pore-size filter into a 72.9 mM NaCl solution, the inferred elongation ratio (vesicle long axis to short axis) is approximately 3.7 ± 0.6. When these vesicles were dialyzed into hypertonic or hypotonic solutions, this elongation ratio varied from 1 (for spherical liposomes) in strongly hypotonic solutions to greater than 6 in increasingly hypertonic solutions, beyond which abrupt morphological transformations appear. These results are quantitatively consistent with a mechanism of vesicle formation by extrusion and with the expectation that vesicle volumes change to equalize internal and external osmolarity via water flow, subject to the constraint of constant bilayer area. Our analysis also provides simplified equations to assess the effects of vesicle elongation and polydispersity on liposome parameters that are commonly required to characterize vesicle preparations for diverse applications. The implications of this study for routine light scattering characterization of extruded vesicles are discussed.

Key words Membrane · Liposome · Morphology · Elongation · Osmotic effect

A.J. Jin (✉)
Laboratory of Physical Biology, NIAMS, Bldg. 6/Rm. 408, NIH, Bethesda, MD 20892-2751, USA
e-mail: ajjin@helix.nih.gov

D. Huster · K. Gawrisch
Laboratory of Membrane Biochemistry and Biophysics, NIAAA, NIH, Rockville, MD 20852, USA

D. Huster
Institute of Medical Physics and Biophysics, University of Leipzig, D-04103 Leipzig, Germany

R. Nossal
Laboratory of Integrative and Medical Biophysics, NICHD, NIH, Bethesda, MD 20892, USA

Introduction

Liposomes (i.e., lipid bilayer vesicles) have received much attention because of their numerous current and potential applications (Ostro 1987; Philippot and Schuber 1995; Lasic and Barenholz 1996; Woodle and Storm 1998). These applications cover areas such as gene therapy and drug delivery vehicles (Allen et al. 1991; Liu et al. 1991; Hontoria et al. 1994; Tabak et al. 1994; Fresta and Puglisi 1997; Hill et al. 1997; Templeton et al. 1997; Walker et al. 1997), food processing microcapsules (Arshady 1993; Fresta et al. 1995), and defined substrates for quantitative basic research (Ertel et al. 1993; Komatsu et al. 1993; Mui et al. 1993; Monshipouri and Rudolph 1995; White et al. 1996; Huster et al. 1997). Among the various methods of liposome preparation, pressure extrusion through polycarbonate filters having uniform circular pores has emerged as a standard procedure, leading to unilamellar vesicles of about 100 nm in diameter. For these stringent applications, characterization of the liposomes has been crucial. Additionally, dedicated liposome characterizations have been explored by many research groups by employing light scattering (Aragon and Pecora 1976; Selser et al. 1976; Hallett et al. 1991; Hallett et al. 1993; Kolchens et al. 1993; Strawbridge and Hallett 1994; Korgel et al. 1998) and other methods including electron micrographic imaging, nuclear magnetic resonance, gel and column filtration, and theoretical inference (Lesieur et al. 1991; Lentz et al. 1992; Winterhalter and Lasic 1993; Choquet et al. 1994).

An important conclusion from these studies is that such extruded liposomes have a rather uniform size distribution, with a small polydispersity that can be readily measured by dynamic light scattering. The extruded liposomes also retain many other desirable features such as a high degree of unilamellar structure, long-term stability, and controlled responsiveness to the environment. As demonstrated by various modeling studies in the applications cited above, knowledge of liposome size and polydispersity is important for quantitative interpretations of results. It is reasonable to expect that vesicle shape, being the other

aspect of vesicle morphology, also may be significant. Although for reasons of simplification it often is assumed that the vesicles are spherical, it has been convincingly argued that liposomes in most applications have various degrees of elongation (Deuling and Helfrich 1976; Lipowski 1991; Seifert et al. 1991; Clerc and Thompson 1994; White et al. 1996). Here we present a combined dynamic and static light scattering method that provides an easy measurement of liposome elongation in addition to the usual measures of mean size and polydispersity. We also show how one can use both aspects of morphological characterizations, i.e., vesicle shape and size, to properly evaluate other liposome parameters. Our results show that liposome elongation has a very significant effect on experimental quantitations in liposome applications, and point to ways to handle such complexity.

A central simplification adopted in our analysis is that the extruded liposomes can be modeled by thin-walled ellipsoidal particles of prolate revolution, with certain distributions in size but a unique elongation ratio. While this ellipsoidal model minimizes the number of essential model parameters, it is comparable to a previously proposed extruded vesicle formation mechanism (Clerc and Thompson 1994) and is in agreement with membrane vesicle properties uncovered over the last decade (e.g., see the review by Seifert and Lipowsky 1996). According to Clerc and Thompson (1994), vesicles from extrusion in osmotic media through 100 nm filter pores arise from uni-bilayer fragments enclosing a reduced internal volume and having the same basic dimensions. Current theoretical understanding and experimental observations offer converging views for vesicle shapes under constraints likely to be encountered during such an extrusion process, but still preclude exact shape expressions. Consequently, any vesicle shape model will necessarily be approximate. Nevertheless, we believe that the ellipsoidal model above is quite good. First, cryo-electron microscopy (EM) visualization of the extruded vesicles in isotonic media often reveal a majority of cylindrical-looking vesicles (e.g., see Mui et al. 1993). While one might have concerns about the fidelity of EM procedures (including the cryo method) and 2D projections of the vesicles from EM are difficult to quantify, such direct visualization is clearly supportive of the adopted model. Second, theoretical shape descriptions from energy minimization suggest that the ellipsoidal shapes are good approximations for extruded vesicles under a broad range of conditions (Seifert 1996; Seifert and Lipowsky 1996; White et al. 1996). Finally, our results and discussion presented in the balance of this paper will further demonstrate that the adopted ellipsoidal model both provides many practical advantages and leads to consistent descriptions of the extruded vesicles for practical applications that are of the main concern here.

In Materials and methods we first revisit the basics of light scattering measurements leading to the mean hydrodynamic radius, polydispersity, and effective radius of gyration of a liposome population. Using analytic expressions compiled in the Appendix, we then explicitly explain our method of combining information about these quantities to evaluate the mean vesicle elongation p^{-1} via a simple equation that is based on modeling liposomes as thin-walled ellipsoidal particles. Two illustrative unimodal size distributions are considered, together leading to the result $p^{-1} = [(R_g + \ell/2)/R_h]\,[1+1.5\,\Delta^2+1.9\,\Delta^4]$, where R_g is the radius of gyration, R_h is the hydrodynamic radius, Δ^2 is the polydispersity, and ℓ is the thickness of the vesicle bilayer. We also demonstrate our scheme of incorporating the effects of vesicle elongation and size distribution by evaluating experimental liposome parameters which are commonly involved in many applications.

The Results section contains experimental results obtained by applying our method to a series of osmotically swollen and shrunken 1-stearoyl-2-oleoyl-*sn*-glycero-3-phosphocholine (SOPC) liposomes produced by extrusion through 100 nm polycarbonate filters in a NaCl solution (72.9 mM). We find that our extruded liposome samples, when suspended in an isotonic medium, have a rather large mean elongation parameter p^{-1} (defined as the ratio of long axis to short axis) of approximately 3.7 ± 0.6, a value that is insensitive to presumed vesicle size distribution functions. We also obtain mean vesicle sizes and size ranges which, however, depend somewhat on specific parameterizations related to the size distribution functions. With these complete morphological properties (elongation, and size with polydispersity), correct values for a number of experimental parameters are produced. We then show that the derived elongation parameter varies from 1 (for spherical liposomes) in strongly hypotonic milieus to larger than 6.0 as the ambient osmotic stress increases to weakly hypertonic, and stays around 5.0 in the highly hypertonic regime. This variation for near-isotonic conditions corresponds to an anticipated linear adjustment of vesicle internal volume, in accordance with the flow of water across the lipid membrane to achieve osmotic balance.

Finally, some Discussion and conclusions, emphasizing the consistency of the proposed approach, are offered. The deduced liposome elongation and osmotic response are found to be consistent with a mechanism of vesicle formation via extrusion proposed by Clerc and Thompson (1994) and SOPC membrane energetic and mechanical behavior under osmotic stress (Needham and Nunn et al. 1990; White et al. 1996; Koenig et al. 1997), and some limitations of this characterization are also noted. This work offers for the first time a complete scheme for obtaining extruded liposome shape elongation, and provides some new insights into the large unilamellar vesicle populations that are most relevant to applications.

Materials and methods

Extrusion of liposomes

The procedure for obtaining extruding liposomes has been described previously (Hope et al. 1985; Mayer et al. 1986; Huster et al. 1997). Briefly, after freezing and thawing five times with liquid nitrogen, SOPC (18 : 0–18 : 1 PC) lipid

samples (Avanti Polar Lipids, Alabaster, Ala.) were prepared at a concentration of 0.7–1.0 wt% in 72.9 mM NaCl by extrusion through polycarbonate filters (Nuclepore, Cambridge, Mass.) in a three-step process (Huster et al. 1997). This extrusion process consists of successively forcing the lipid sample three times through 400 nm filters, followed by three passages through 200 nm filters and six passages through 100 nm filters, always under argon gas pressure. The final extruded SOPC samples, which appeared to be translucent, were dialyzed overnight against NaCl solutions of molality varying from 12 mM to 150 mM. Before performing light scattering characterizations, dilutions of the samples were performed 10- to 100-fold by adding a measured amount of sample to the corresponding dialysis solution.

Dynamic and static light scattering

Morphological characteristics of lipid vesicles were assessed by light scattering measurements. Measurements for various vesicle samples, at typical lipid concentrations of 0.01% by weight, were carried out on a BIC light scattering spectrometer (Brookhaven Instrument, Holtsville, New York) consisting of a model BI-200SM goniometer, an EMI-9863 photomultiplier tube (PMT), a BI-9000AT digital correlator, and a Lexel 95-21 argon ion laser operated at a wavelength of 514.5 nm and power of 100 mW. The scattering cell was immersed in a refractive index matching fluid whose temperature was controlled at 25± 0.1 °C. Data for dynamic and static scattering were collected simultaneously, and later analyzed with software supplied with the instrument. For each sample, data were acquired – typically for a duration of 15 min – for 1–3 runs at angles 30°, 45°, 60°, 90°, 120°, and 150°. The count rate was monitored to exclude runs containing artifacts due to infrequent passage of dust particles through the scattering volume.

Static light scattering intensities were corrected for background/solvent contributions and PMT dead-time, and normalized with respect to scattering from spectrophotometric-grade benzene. This normalized scattering intensity is the Rayleigh ratio, $I_s(Q)$, where $Q = 4\pi n \lambda^{-1} \sin(\theta/2)$ is the magnitude of the scattering-angle-dependent wave-vector. The $I_s(Q)$ were classically analyzed (e.g. Nossal et al. 1983; Schmitz 1990; White et al. 1996) via

$$[I(Q)/I(0)]^{-1/2} = 1 + Q^2 \langle R_g^2 \rangle_z / 6 + o(Q^4) \quad (1)$$

which yields the scattering-intensity averaged ("Z-averaged") radius of gyration, $\langle R \rangle_g \equiv (\langle R_g^2 \rangle)^{1/2}$ (see Fig. 1). For extruded liposomes of about 50 nm in radius, the higher order terms, $o(Q^4)$, etc., are negligible. Other studies carried out in our laboratory indicate that weak vesicle aggregation, possibly present because the scattering samples were of finite lipid concentration, is inconsequential at the concentrations used here.

The autocorrelation function $g_1(\tau)$, given as a function of delay time τ, was independently fitted at each scattering angle using histogram methods (e.g. "CONTIN", BI-9000AT Instrument Manual, Brookhaven Instrument; Dahneke 1983). We thereby verified that the distributions of the suspended lipid vesicles essentially were unimodal. Consequently, the autocorrelation function was fitted by a second-order cumulants expansion (see Fig. 2)

$$\ln|g_1(\tau)| = -(\langle D \rangle_z Q^2)\,\tau + (\mu_z Q^4/2)\,\tau^2 + o(\tau^3) \quad (2)$$

which yielded the Z-averaged and rotationally averaged apparent translational diffusion coefficient $\langle D \rangle_z$ and second moment μ_z (Nossal et al. 1983; Dahneke 1983; Schmitz 1990). Then, for each scattering angle, the Z-averaged, apparent hydrodynamic radius $\langle R_h \rangle_z$ was calculated via

$$\langle R_h \rangle_z = k_B T / (4\pi \eta_s \langle D \rangle_z) \quad (3)$$

where k_B is the Boltzmann constant, T is the absolute temperature, and η_s is the solvent viscosity. Also, we obtained

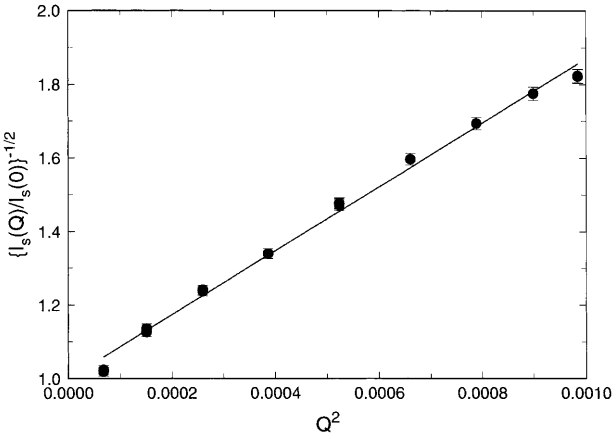

Fig. 1 Typical static light scattering intensities, plotted as $I_s(Q)^{-1/2}$ vs Q^2, where Q is the magnitude of the Bragg scattering vector. In accord with Eq. (1), linear fits yield the Z-averaged square radius of gyration, $\langle R_g^2 \rangle_z$. Data are for the "standard sample," i.e., vesicles suspended in an isotonic, 72.9 mM NaCl solution

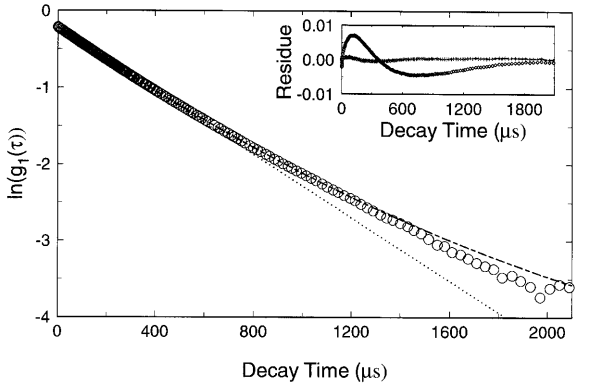

Fig. 2 Typical photon autocorrelation function, $g_1(\tau)$, fitted (*dashed line*) according to a second-order cumulant expansion as given in Eq. (2). (For comparison, the *dotted line* shows a single exponential fit, obtained by setting $\mu_z = 0$.) The high quality of the cumulant fit, as indicated in the inset by the residuals to the fit, indicate a relatively narrow, unimodal vesicle size distribution. The *inset* shows the $g_1(\tau)$ residues of the cumulant fit (+) and the single exponential fit (◇). Data for 90° scattering angle, standard 72.9 mM NaCl sample

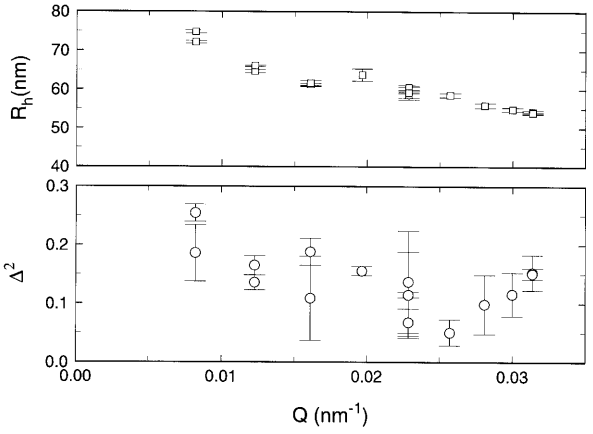

Fig. 3 Typical scattering wave-vector dependence of the reduced hydrodynamic radius $\langle R_h \rangle_z$ [*squares*, see Eq. (3)] and polydispersity Δ_z^2 [*circles*, see Eq. (4)] with uncertainty derived from cumulant fits. Data are for standard 72.9 mM NaCl vesicle suspension

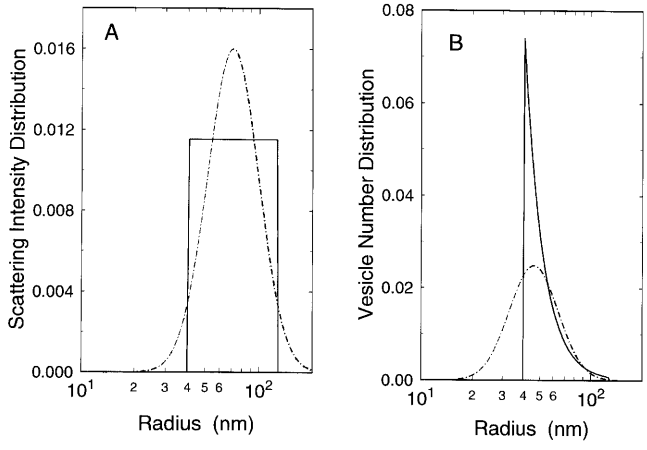

Fig. 4A, B Examples of vesicle size distribution functions $\mathfrak{p}(R_s)$ obtained by assuming a square-distribution [*dashed line*, see Eq. (A10)] or log normal distribution [*solid line*, see Eq. (A9)]. The parameters $\{R_{0h}, \delta\}$ and $\{\tilde{R}_0, \tilde{\delta}\}$ are those which are obtained for the standard 72.9 mM NaCl sample (see below). Intensity weighted distributions are shown in **A**, and corresponding number distributions appear in **B**

the convenient quantity Δ_z which is related to μ_z by

$$\Delta_z^2 \equiv \mu_z / \langle D \rangle_z^2 = (\langle 1/R_h^2 \rangle_z - \langle 1/R_h \rangle_z^2) / \langle 1/R_h \rangle_z^2 \tag{4}$$

Values of $\langle R_h \rangle_z$ and Δ_z^2, for a typical sample, are shown as functions of Q in Fig. 3. Note that Δ_z^2 usually falls within the range 0.1–0.2, signifying that the underlying unimodal size distribution is relatively narrow. This measure of polydispersity seems to have no significant dependence on Q in the present investigation. However, the apparent hydrodynamic radius $\langle R_h \rangle_z$ shows a slight dependence on scattering angle (see Fig. 3). In a subsequent analysis, we propose to take $\langle R \rangle_h$ and Δ^2 for each sample to be an error-weighted average of the $\{\langle R_h \rangle_z\}$ and $\{\Delta_z^2\}$ measured at the various angles.

Determination of vesicle elongation

The above-described light scattering measurements provide one set of data, $\langle R \rangle_g$, $\langle R \rangle_h$, and Δ^2. These quantities depend on, and are averaged over, the shape and size distributions of the vesicles in the sample suspension. To produce the vesicle parameters of interest, we model these liposomal vesicles as thin-wall prolate ellipsoids by two alternative size distributions and a constant elongation. In the Appendix, we have presented basic expressions for ideal ellipsoids, the effects of the two size distributions [i.e., a log-normal distribution $\mathfrak{p}^{LN}(R; R_0, \delta)$ or a square-wave distribution $\mathfrak{p}^{SW}(R; \tilde{R}_0, \tilde{\delta})$; see Eqs. (A9) and (A10) and Fig. 4], and the corrections due to the finite bilayer thickness [Eqs. (A1)–(A14)]. The rational for this ellipsoidal model is presented in the Introduction and further addressed in the Discussion section.

Combining these basic equations for ideal ellipsoidal vesicles, size-distribution and thin-wall corrections, we can now obtain the basic equation for vesicle morphology. It follows, by rearranging Eqs. (A6), (A7), and (A13) or (A14), that the average shape of the vesicle can be assessed via the ratio

$$\frac{f_g(p)}{f_h(p)} = \rho_e \equiv \rho_L \, \beta^M(\Delta) \tag{5}$$

where

$$\rho_L \equiv \frac{\langle R \rangle_g + \ell/2}{\langle R \rangle_h} \quad \text{and} \quad \beta^M(\Delta) \equiv \left[\frac{\alpha_4 (\Delta)^3}{\alpha_3 (\Delta)^2 \, \alpha_6 (\Delta)} \right]^{1/2} \tag{6}$$

are available directly from the combined dynamic and static light scattering measurements. For our examples of log-normal or square-wave size distribution [Eqs. (A9) and (A10)], the vesicle morphology is affected via the term [after using Eqs. (A11)–(A14)]

$$\beta^{M=LN}(\Delta) = (1+\Delta^2)^{-3/2} = 1 - \frac{3}{2}\Delta^2 + \frac{15}{8}\Delta^4 + O(\Delta^6)$$
$$\cong 1 - \frac{3}{2}\Delta^2 + 1.5\,\Delta^4 \tag{7}$$

or

$$\beta^{M=SW}(\Delta) = 1 - \frac{3}{2}\Delta^2 + \frac{147}{40}\Delta^4 + O(\Delta^5)$$
$$\cong 1 - \frac{3}{2}\Delta^2 + 2.3\,\Delta^4 \tag{8}$$

respectively, where the leading order Δ^2-terms agree with each other but the coefficients of the Δ^4-terms – which were determined from best truncation approximations to the two respective model size distributions (via TableCurve 2D, Jandel Scientific Software) – differ slightly. Since the explicit forms of $f_g(p)$ and $f_h(p)$ are defined in Eqs. (A1) and (A2), the vesicle elongation parameter p^{-1} can be deduced from Eq. (5) by following any standard method of solving nonlinear equations. To make this process more convenient, we have discovered (again via TableCurve 2D) an ex-

ceedingly good approximate solution to be

$$p^{-1} \cong 1 + 9.3 \sqrt{\frac{(\rho_e - 1)}{-\ln(\rho_e - 1)}} \quad \text{with}$$
$$\rho_e \cong \frac{\langle R \rangle_g + \ell/2}{\langle R \rangle_h} \left[1 - \frac{3}{2} \Delta^2 + 1.9 \Delta^4 \right] \tag{9}$$

where the coefficient of the Δ^4-term is adopted to reflect the average over the small differences between the log-normal and square-wave distribution. This expression provides p^{-1} values in the range $1 \le p^{-1} < 7$ for values $1 \le \rho_e < 1.4$ and $0 \le \Delta^2 < 0.3$, covering the range of liposome morphology that turns out to be most relevant. For any given (ρ_e, Δ) within that range, differences between the calculated values of p^{-1} are only a few percent when using either the exact functions of $f_h(p)$ and $f_g(p)$ or the Δ^4-terms specific to the distributions $\mathfrak{p}^{LN}(R)$ and $\mathfrak{p}^{SW}(R)$. If $\rho_e \le 1$, spherical liposomes corresponding to $p^{-1} = 1$ can be presumed.

Calculation of vesicle size parameters and entrapped volume

The above derivations, leading to the determination of the elongation parameters, show that one must carefully identify each liposome size parameter in order to provide any meaningful values. Staying with the log-normal or square-wave distributions [Eqs. (A9) and (A10) for equations], the size range of liposomes most responsible for the light scattering intensity may be characterized either as lying within the range ($R_0\, e^{-\delta}$, $R_0\, e^{\delta}$) with the geometric mean of R_0, or within [$\tilde{R}_0$, $\tilde{R}_0(1+\tilde{\delta})$] with the geometric mean of $\tilde{R}_0 \sqrt{1+\tilde{\delta}}$, respectively [see Eqs. (A9) and (A10) and Fig. 4]. Then Eqs. (A11) and (A12) allow the evaluations of the distribution width factors

$$\delta = \sqrt{\ln(1+\Delta^2)} \quad \text{and} \quad \tilde{\delta} \cong \sqrt{12\,\Delta^2 + (15.5\,\Delta^2)^2} \tag{10}$$

For the mean distribution size, one obtains, by rearranging Eqs. (A7) and (A13) or Eqs. (A12) and (A14)

$$R_0 = \frac{1}{f_h(p)} \frac{\alpha_3^{LN}(\Delta)}{\alpha_4^{LN}(\Delta)} \langle R \rangle_h \cong \frac{1 - 0.05\,(p^{-1} - 1)}{\sqrt{1+\Delta^2}} \langle R \rangle_h$$
$$\tilde{R}_0 = \frac{1}{f_h(p)} \frac{\alpha_3^{SW}(\Delta)}{\alpha_4^{SW}(\Delta)} \langle R \rangle_h \tag{11}$$
$$\cong \frac{1 - 0.05\,(p^{-1} - 1)}{\sqrt{(1+\Delta^2)\,(1+\sqrt{12\,\Delta^2 + (15.5\,\Delta^2)^2})}} \langle R \rangle_h$$

where very good approximate expressions for $f_h(p)$ and $\alpha_n^{SW}(\Delta)$ have been introduced (via Table Curve 2D) for the relevant liposome parameter values, $1 \le p < 7$ and $\Delta^2 < 0.3$. Note from the above that $R_0 = \tilde{R}_0 \sqrt{1+\tilde{\delta}}$, i.e., that the geometric means of the two distributions coincide with each other.

The expressions given in Eq. (11) are intensity weighted measures of mean vesicle size. If one's experimental applications require the size range of liposomes *that are most numerous*, the characteristic liposome sizes have to be derived from the number distributions and will move to smaller values. Taking the log-normal distribution as the example, this size range for liposome particle number becomes ($R_{0N}\, e^{-\delta}$, $R_{0N}\, e^{\delta}$) with the center (geometric mean) value shifted to the smaller value $R_{0N} = R_0 \exp(-4\,\delta^2)$. Similarly, the number distribution corresponding to the square-wave shows a sharp cutoff at the lower limit, $\tilde{R}_0$, and decays to less than e^{-1} of maximum probability for $R_s > \tilde{R}_0\, e^{1/4}$, so it also reflects a shift to smaller sizes (see Fig. 4). Thus, especially when the polydispersity is small, the two illustrative distributions possess many mutually consistent features that should be taken seriously. The different distribution forms can be thought of as alternative parametrizations of the size range for the vesicle population. Combining these parameterized size ranges with mean elongation allows evaluation of related parameters such as the mean long-axis dimension, $a_0 = R_0\, p^{-2/3}$, and short-axis dimension, $b_0 = R_0\, p^{1/3}$.

Another liposome parameter common to a number of applications is the *vesicle entrapped volume*, V_e, i.e. the total internal volume of vesicle per unit lipid mass (e.g., see Huster et al. 1997, where this quantity is used to quantify water permeation rate across bilayers). We take this as our final example of liposome parameters where valuations are significantly affected by vesicle morphological factors for which we must carefully include corrections from liposome size distribution and bilayer thickness. Because, for a given lipid, the surface area occupied by each molecule, A_L, is approximately independent of vesicle shape and size, this entrapped volume is proportional to the liposome radius parameter introduced before, in Eq. (A4), as

$$V_e \equiv \frac{V}{M_L\,(2\,A/(A_L\,N_A))} = R_e\,\frac{A_L\,N_A}{6\,M_L} \tag{12}$$

Here, as previously, A is the vesicle surface area, V is vesicle internal volume, M_L is the molar mass of the lipid, and N_A is the Avogadro's number. For liposomes with a narrow size distribution and thin walls, the relevant averaged quantity denoted as $\langle V \rangle_e$ can be calculated according to $\langle V \rangle_e \propto \langle R \rangle_e \equiv 3\,(\int V)/(\int A)$ (Huster et al. 1997). Thus, by a derivation similar to that which gave rise to Eq. (A7) for $\langle R \rangle_h$, we find that the parameter pair $\{\langle R \rangle_e, \langle V \rangle_e\}$ may be related to the elongation p^{-1} and the moments $\langle R_s^n \rangle$ as

$$\langle R \rangle_e \equiv \langle V \rangle_e \frac{6\,M_L}{A_L\,N_A} = \left[\frac{3 \int [V(R_s, p)]\,\mathfrak{p}(R_s)\,dR_s}{\int [A(R_s, p)] \cdot \mathfrak{p}(R_s)\,dR_s} \right]$$
$$= f_e(p) \frac{\langle R_s^3 \rangle}{\langle R_s^2 \rangle} - 2\,\ell \tag{13}$$

In the above, the effect of substracting $2\,\ell \simeq 8.0$ nm from bilayer thickness for a thin-wall correction approximately takes into account both the adjustment of $-3\,\ell$ for the volume (from the inner to the outer surface) and the adjustment of 2 ($\ell/2$) for the area (from the middle to the outer surface). Such first-order approximation for the thin-wall correction is sufficient because its magnitude is still small

[see discussion following Eq. (A14)]. Therefore, by using Eqs. (A7) and (A8), one gets the expression

$$\langle R\rangle_e = \frac{f_e(p)}{f_h(p)}\frac{\langle R\rangle_h}{1+\Delta^2} - \ell \cong \left[1 - \frac{011\,(p^{-1}-1)^2}{1+0.6\,(p^{-1}-1)\ln(p^{-1}-1)}\right]\frac{\langle R\rangle_h}{1+\Delta^2} - 2\,\ell \quad (14)$$

Note that this equation happens to be independent of any assumed form for the size distribution, with the effect of vesicle polydispersity accounted for by the factor $(1+\Delta^2)$. The vesicle elongation affects $\langle R\rangle_e$ via the ratio $f_e(p)/f_h(p)$, which can calculated exactly from the definitions given by Eqs. (A1) and (A4); we find that the approximate expression given in the bracket in Eq. (14) deviates less than 3% from its true value for the relevant range of liposome morphology $1 \le p^{-1} < 7$, for which we find that $1 \le f_e(p)/f_h(p) < 0.45$.

Results

The above-described light scattering measurements and data reduction methods demonstrate that the vesicle parameters of interest – mainly the mean vesicle elongation and size range – can be determined from analyzing light scattering data and be used to infer experimentally relevant quantities like vesicle entrapped volume. We have applied our characterization method to three sets of SOPC liposome samples produced by repeated extrusions of SOPC lipid – suspended in a 72.9 mM NaCl solution – through 100 nm pore-size polycarbonate filters (see Materials and methods). Table 1 contains the light scattering results and various derived elongation and other parameters for liposome samples diluted into an isotonic medium. In addition, results are given for aliquots of these samples that were dialyzed overnight against NaCl solutions of molarity varying from 12 mM to 150 mM. The osmotic responses of liposome morphology are shown in Figs. 5 and 6.

Table 1 Liposome morphological parameters in an isotonic medium (s.d. = standard deviation based on three data sets; see the text for notations)

(A) Combined light scattering measurements	
Radius of gyration, $\langle R\rangle_g \pm$s.d.	98±13 (nm)
Hydrodynamic radius $\langle R\rangle_h \pm$s.d.	69±9 (nm)
Polydispersity, $\Delta^2 \pm$s.d.	0.16±0.03
(B) Calculated morphological parameters	
Liposome elongation, $p^{-1} \pm$s.d.	3.7±0.6
Radius distribution (log-normal), $\{R_0\,e^{-\delta}, R_0, R_0\,e^{\delta}\}$	38, 56, 82 (nm)
Radius distribution (square-wave), $\{\tilde{R}_0, \tilde{R}_0\sqrt{1+\tilde{\delta}}, \tilde{R}_0(1+\tilde{\delta})\}$	29, 56 109 (nm)
(C) Inferred liposome parameters	
Shape functions, $f_h(p)$, $f_g(p)$	1.16, 1.35
Shape functions, $f_A(p)$, $f_v(p)$	1.25, 1.40
Liposome long-axis, $a_0 \equiv R_0\,p^{-2/3}$	134 (nm)
Liposome short-axis, $b_0 \equiv R_0\,p^{1/3}$	36 (nm)
Size distribution for vesicle number	
(log-normal: $\{R_{0N}\,e^{-\delta}, R_{0N}, R_{0N}\,e^{\delta}\}$	21, 31, 45 (nm)
(square-wave: $\{\tilde{R}_0, \tilde{R}_0\,e^{1/8}, \tilde{R}_0\,e^{1/4}\}$	29, 33, 37 (nm)
Entrapment radius $\langle R\rangle_e \pm$s.d.	38±7 (nm)
Entrapped volume $\langle V\rangle_e \pm$s.d.	2.7±0.6 (μl/mg)

Liposome morphology in isotonic milieu

Combined dynamic and static light scattering measurements on each sample directly yield three characterization parameters, $\{\langle R\rangle_g, \langle R\rangle_h, \Delta^2\}$, i.e., the radius of gyration, hydrodynamic radius, and polydispersity, respectively (see Materials and methods and Figs. 1–3). We find, for three sets of samples diluted in an isotonic milieu, $\langle R\rangle_g = 98 \pm 13$ nm, $\langle R\rangle_h = 69 \pm 9$ nm, and $\Delta^2 = 0.16 \pm 0.03$ nm, where the variations noted by the standard deviations are indicative of sample differences as well as light scattering measurement inaccuracies (Table 1). These results agree with the expectation that the liposomes have relatively uniform sizes comparable to that of the filter pore. The difference between $\langle R\rangle_g$ and $\langle R\rangle_h$ is quite noticeable, and demonstrate that one must refer to specific size parameters in addressing questions like "what is the vesicle size?".

Following our analysis scheme (see Materials and methods), liposome shape and size distributions can be determined from the set of light scattering results, $\{\langle R\rangle_g, \langle R\rangle_h, \Delta^2\}$. We find these extruded liposomes in isotonic milieu to be decidedly non-spherical with mean elongation ratio (i.e., prolate ellipsoidal long axis to short axis ratio) of $p^{-1} = 3.7 \pm 0.6$ [Eq. (9) and Table 1]. When the liposome sizes are parameterized by the equivalent spherical radius R_s (i.e., the radius of a sphere with an equal volume), we find that the light intensity is most probably scattered from liposomes having $R_s \cong R_0 = 56$ nm. The liposome size range for the scattering intensity can be parameterized either by a log-normal distribution [Eq. (A9)] with the standard deviation lower and upper limits of $\{R_0\,e^{-\delta}, R_0\,e^{\delta}\} = \{38, 82\}$ nm, or by a square-wave distribution [Eq. (A10)] with the lower and upper cutoff limits of $\{\tilde{R}_0, \tilde{R}_0(1+\tilde{\delta})\} = \{29, 109\}$ nm (see Fig. 4 and Table 1).

To use the determined liposome morphological characterizations in other applications, we stress that one must critically evaluate the given application to determine those parameters that are truly relevant for particular quantitations (see Materials and methods). Owing to the non-sphericity of the extruded vesicles in an isotonic milieu, these relevant parameters will involve shape functions like $f_h(p)$, $f_g(p)$, $f_A(p)$ and $f_V(p)$ [see Eqs. (A1)–(A5), etc.]. The highly non-spherical liposome shape means that the experimentally inferred shape functions deviate noticeably from unity (Table 1). Although the central equivalent spherical radius R_0 is very close to the filter pore radius of about 50 nm, the central long-axis radius and short-axis radius of the sample, $\{a_0, b_0\} = [134, 36\}$ nm, differ consid-

erably from R_0. In applications where the liposome size range for particle numbers is relevant, our approach suggests that the largest portion of liposomes have $R_s \cong R_{0N} =$ 32 nm. When the vesicle number distribution is parameterized either by a log-normal distribution or by a square-wave distribution, the lower and upper limits of the equivalent radius for the majority of the vesicles are about 29 nm and 37 nm, respectively (see Fig. 4 and Table 1). This size shift between the vesicle number distribution and the scattering intensity distribution correlates with the observed size polydispersity for the extruded vesicles. Although small, it nevertheless must be accounted for.

Finally, we apply the analysis in Materials and methods to the evaluation of a pair of related entrapped volume parameters, $\{\langle R\rangle_e, \langle V\rangle_e\}$, relevant to a vesicle permeation study (Huster et al. 1997). The final results, inferred directly from our light scattering data [see Eqs. (13) and (14)], are $\langle R\rangle_e = 38 \pm 7$ nm and $\langle V\rangle_e = 2.7 \pm 0.6$ µl/mg, where the variations are standard deviations from the three sample sets (Table 1). The values $M_L = 824.16$ for the molar mass and $A_L = 0.666$ nm^2 for the monolayer area per lipid of SOPC, used for calculating $\langle V\rangle_e$ from $\langle R\rangle_e$ via Eq. (14), were adopted from the literature (Huster et al. 1997).

Osmotic effect

Figure 5 shows the deduced elongation parameter, p^{-1}, for aliquots of the extruded samples that were dialyzed overnight in hypo- and hyper-osmotic NaCl solutions (A), together with ratio ρ_L and the polydispersity Δ^2 (B). The elongation values in Fig. 5a were inferred from the light scattering measurements in Fig. 5B according to Eqs. (6) and (9). The polydispersity value Δ^2 shows no appreciable change related to dialysis for the entire ambient osmotic concentration range of 12 mM $\leq$ [NaCl] $\leq$ 150 mM, and always is close to 0.14 (with a standard deviation of 0.02 for 18 sample sets, including the three involving an isotonic milieu). The elongation parameter p^{-1}, on the other hand, tracks the ratio ρ_L [evaluated via Eq. (6)], which varies due to changes in the $\langle R\rangle_g$ and $\langle R\rangle_h$ that occur when the extruded vesicles are dialyzed. For hypotonic media with [NaCl] $\lesssim$ 40 mM, the resulting elongation of $p^{-1} \cong 1$ implies that the vesicles have become spherical. When ambient osmolarity is increased beyond that of the isotonic NaCl concentration ($[NaCl]_0 = 72.9$ mM), the vesicles become more elongated and reach a value of $p^{-1} \cong 6$ near [NaCl] = 90 mM. For yet stronger hyper-osmotic milieus, the derived elongation parameter settles around $p^{-1} \cong 5$.

Figure 6 shows the corresponding values of the relative volume ratio $f_V(p)$ as a function of the osmotic stress ratio $[NaCl]/[NaCl]_0$. The ratio $f_V(p)$ has been calculated via Eq. (5) to emphasize the difference between actual vesicle volumes and those of spherical vesicles having the same bilayer surface areas. This shows more distinctly the three regimes of behavior: (I) spherical vesicles for hypotonic milieu, with $[NaCl]/[NaCl]_0 \lesssim 0.6$; (II) elongated vesicles with linear osmotic response in the isotonic neighborhood,

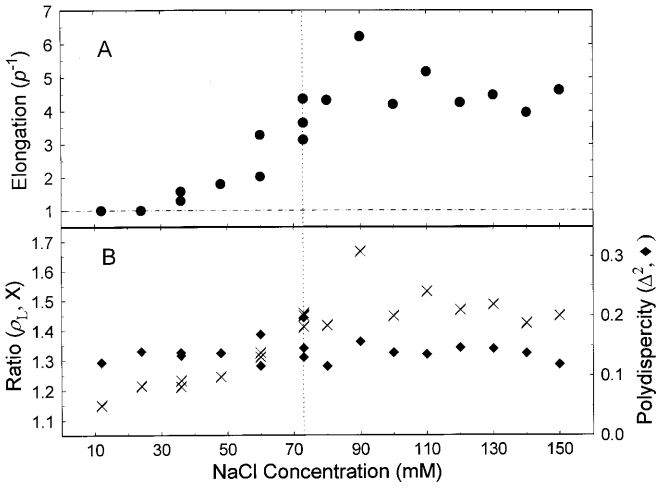

Fig. 5A, B Shape change induced by dialysis of vesicles into hypo- or hypertonic media: **A** inferred elongation parameter, p^{-1}; **B** parameters ρ_L and Δ^2, determined from light scattering and used to calculate p^{-1} according to Eqs. (5), (6), and (9). Isotonic condition (72.9 mM NaCl) is indicated by the *vertical line*

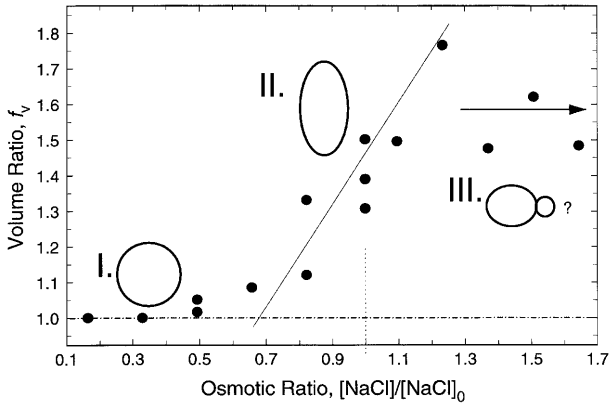

Fig. 6 Variation in relative vesicle volume due to change in elongation arising from vesicle swelling or shrinkage in hypo- or hypertonic media. f_V, defined in Eq. (A5) as the inverse ratio of liposome volume to that of a hypothetical spherical vesicle having the same surface area, is a simple measure of vesicle non-sphericity. This volume ratio, f_V, is related via a simple fractional power-law to an area ratio, f_A [see Eq. (A5)], measuring the relative excess of the vesicle surface over that of an equal volume sphere. The three regimes of behavior are discussed in the text. Isotonic condition corresponds to $[NaCl] = [NaCl]_0 = 72.9$ mM

with $1.0 \lesssim f_V(p) \lesssim 1.8$ and $0.7 \lesssim [NaCl]/[NaCl]_0 \lesssim 1.2$; and (III) elongated vesicles with non-linear osmotic response, with $[NaCl]/[NaCl]_0 \gtrsim 1.3$. (Note that the line fitted through regime II has only one adjustable parameter, as it was constrained to pass through the coordinate origin.) This is quantitatively in accord with the notion that vesicles in the isotonic neighborhood always achieve osmotic stress balance by adjustment of the internal NaCl concentration (via water flow across the bilayer) to that of the dialysis milieu.

Discussion and conclusions

Consistency of the results

The isotonic results and osmotic effects, taken together, provide consistency support for the validity of the present approach for liposome characterization. The deduced nonspherical nature and size distribution of the liposomes extruded in osmotic solutions is expected from a mechanism for extruded vesicle formation proposed by Clerc and Thompson (1994). Membrane fragments are envisioned to assume long cylindrical shapes during the pressure-driven extrusion, and to slide with viscous flow along the straight pores of the polycarbonate filters. Because of a well-known fluctuation instability (Walstra 1983), the long cylindrical membrane fragment will break periodically into a string of elongated cylinders, each having the length of $\lambda \cong 2\,\pi r$, where r is the radius of the cylinder. We believe that, after such breakage, the membrane cylinders reseal to eliminate free edges that are energetically costly, thereby trapping within a cylindrical volume of osmotic fluid. Because of the requirement to balance the osmotic stress across the bilayer, the sealed vesicles are under constraints of both surface area and internal volume, and may not be able to adjust their shape greatly even after emerging from the pores. Thus, typical liposomes should maintain an elongated shape with the volume ratio value of

$$f_V \cong \frac{(4\,\pi/3)\,(A_C/4\,\pi)^{3/2}}{V_C} \cong 1.475 \tag{15}$$

which is evaluated from the cylinder surface area of $A_C = 2\,\pi r\,\lambda + 2\,\pi r^2$ and volume of $V_C = \lambda\,\pi r^2$ together with the instability condition, $\lambda \cong 2\,\pi r$ [see Eq. (A5)].

The above mechanism therefore predicts that all the extruded vesicles should have the same degree of non-sphericity, although their short-axis radius varies within a size range that is somewhat smaller than the slightly dispersed filter pore sizes of approximately 50 nm. The morphological results deduced from our three isotonic samples matches these predictions extremely well. The volume ratio f_V, that was inferred via Eq. (A5) from the stated elongation parameter $p^{-1} = 3.7 \pm 0.6$, has a mean value of 1.4 (in Table 1), close to the value of about 1.5 extrapolated from the data shown in Fig. 6. Both values are in close agreement with the prediction given in Eq. (15). These f_V values correspond well with the observation that the liposome internal volume is about 30–40% less than the maximum spherical volume allowed by its surface area (Clerc and Thompson 1994; Huster et al. 1997). The inferred size ranges, expressed in terms of equivalent spherical radius, and the corresponding long-axis and short-axis radii, are also very reasonable in comparison with the filter pore size distribution available from the manufacture (Nuclepore, Cambridge, Mass.).

The behavior of $f_V(p)$ shown in Fig. 6, and the implied liposome morphological changes upon liposome osmotic dialysis, are *quantitatively* in accord with the following osmotic stress response mechanism (White et al. 1996) in which vesicle internal volumes change in order that the liposome interiors be in osmotic balance with the exterior dialysis milieu. The osmotic pressures of the NaCl solutions are given by the standard equation (e.g. Rock 1969)

$$\pi_{os}([\mathrm{NaCl}]) = -\frac{R_{gas}\,T}{V^0_{H_2O}} \ln(X_{H_2O}) \approx (0.049\ \mathrm{atm})\,\frac{[\mathrm{NaCl}]}{mM} \tag{16}$$

where R_{gas}, $V^0_{H_2O}$, $X^0_{H_2O}$, and T are the molar gas constant, the molar volume of the water, the mole fraction of the water, and the ambient temperature, respectively. On the other hand, the membrane bending elastic energy, with which liposomes maintain their morphology, is adequately given by the Helfrich "effective Hamiltonian" of the form

$$H_B = \oint dA \left\{ -k\,C_0(C_1 + C_2) + \frac{1}{2}\,k\,(C_1 + C_2)^2 + k_G\,C_1\,C_2 \right\} \tag{17}$$

where C_1 and C_2 are two principle curvatures and C_0, k, and k_G are the spontaneous curvature, bending rigidity, and gaussian curvature modulus (Deuling and Helfrich 1976; Lipowsky 1991; Seifert and Lipowsky 1996). Because the gaussian curvature term remains constant upon integration, the change in bending energy for each vesicle corresponding to shape change is of the order of the bending energy for spheres with zero spontaneous curvature, i.e., $\Delta H_B = 8\,\pi\,k \le 2 \times 10^{-18}$ J, where $k = 10 - 20\ K_B T$ is used for a typical membrane formed by lipids like SOPC (Lipowsky 1991). For an extruded liposome having equivalent spherical radius $R_s = 50$ nm, this bending elastic energy equals the osmotic deformation energy, $\Delta H_\pi = \pi_{os}(\Delta[\mathrm{NaCl}])\,(4\,\pi/3)\,R_s^3$, when the concentration difference across the bilayer is $\Delta[\mathrm{NaCl}] = 0.03$ mM. Therefore, within our osmotic stress range of 12 mM < [NaCl] < 150 mM, nonspherical liposomes must always have their internal NaCl concentration adjusted to that of the dialysis milieu.

Because Na^+ and Cl^- ions cannot diffuse across an intact SOPC membrane, the internal NaCl concentration changes only via water permeation across the membranes. When the osmolarity of the ambient solution is decreased or increased, liposomes expand to become more spherical or shrink to become more elongated. Quantitatively, one expects that the internal vesicle volume of each vesicle scales inversely with its final [NaCl] and, hence, the volume ratio behaves as

$$f_V = f_{V0}\,\frac{[\mathrm{NaCl}]}{[\mathrm{NaCl}]_0} \tag{18}$$

where f_{V0} is the volume ratio in an isotonic milieu for which $[\mathrm{NaCl}] = [\mathrm{NaCl}]_0$. However, when the osmolarity of the ambient solution is decreased greatly such that $[\mathrm{NaCl}] < [\mathrm{NaCl}]_0/f_{V0}$, liposomes which are already fully swollen may withstand a certain amount of osmotic stress before experiencing lysis (Needham and Nunn 1990; Ertel et al. 1993; Mui et al. 1993; Koenig et al. 1997). Membrane expansion and breakage can be quantitatively estimated via the standard Laplace's law

$$\tau = \Delta\pi_{os}\,r/2 \tag{19}$$

where τ is lateral tension experienced by the spherical vesicle of radius r that are fully swollen under the osmotic stress $\Delta\pi_{os}$ across the bilayer. For SOPC membranes, an elastic tensile strength of $\tau_{lys} = 5.7$ dyn/cm was previously estimated (Needham and Nunn 1990). Therefore, for vesicles of 50 nm spherical radius, the membrane can withstand an ambient NaCl concentration that is lower than that of the internal volume by as much as $\Delta[\mathrm{NaCl}]_{lys} \cong [(2\ \tau_{lys}/r)/0.049\ \mathrm{atm})]$ mM $\cong$ 46 mM, as derived from Eqs. (16) and (19). Larger vesicles can withstand proportionally lower values of $\Delta[\mathrm{NaCl}]_{lys}$.

If $\Delta[\mathrm{NaCl}]_{lys}$ is surpassed, vesicles experience lysis to release some of their osmotic components and then reseal into vesicles that are essentially spherical, for which one expects a constant value $f_V = 1$. On the other hand, under a sub-lysis lateral tension of $\tau < \tau_{lys}$, SOPC membrane area expansion and its thickness reduction will be fairly insignificant because of the large membrane lateral compressibility moduli (Koenig et al. 1997). In either case, liposomes will remain as spherical vesicles of similar radii when the ambient osmolality decreases below the point of full swelling at $[\mathrm{NaCl}] = [\mathrm{NaCl}]_0/f_{V0}$.

Our data for volume fraction in Fig. 6 are fully consistent with the above interpretation for both in the hypotonic regime (I) and in the near isotonic regime (II). A straight line fits the data of regime II (values $1.0 \le f_V < 1.8$ and $50 < [\mathrm{NaCl}] < 90$ mM) with only one adjustable parameter according to Eq. (18). Because $[\mathrm{NaCl}]_0/f_{V0} \cong 49$ mM and most of the liposomes in our samples have radii smaller than 100 nm (Table 1), a large majority of vesicles will not experience lysis in our hypotonic media in regime I. Correspondingly, the elongation factor p^{-1} varies over the range from 1 to 6 (see Fig. 5). For regime III in hypertonic dialysis solutions ($[\mathrm{NaCl}] > 100$ mM), for which the vesicle internal volume would have dropped to less than half of the allowed spherical volume, the data show a break in pattern. We believe that the pattern break suggests that vesicle morphology changes from that of a prolate ellipsoid of revolution to a more complicated structure for which our morphological relations no longer apply. The insets in Fig. 6 depict likely shapes of typical extruded vesicles. Such shape transition at highly reduced internal entrapped volume is expected from the viewpoint of bilayer shape energy minimization (Deuling and Helfrich 1976; Lipowsky 1991; Seifert 1996; Seifert and Lipowsky 1996). Although the noise in the experimental data is fairly large, the transition boundary is probably around $f_V = 1.7 \pm 0.2$, i.e. when the internal volume reduction reaches around 41% of the maximal spherical volume. This transition point corresponds [via Eq. (A5)] to a membrane surface area that is about 41% in excess of its minimal need for enclosing the reduced volume. These transition boundary values may be somewhat higher than some earlier experimental observations (e.g. Kas and Sackmann 1991; Farge and Devaux 1992) that, however, are mostly for micrometer and larger membrane vesicles and may involve different constraints.

In a previously reported study (Huster et al. 1997), a pair of entrapped volume parameters $\{\langle R\rangle_e, \langle V\rangle_e\}$ was assessed for the quantitation of water permeation rates across bilayers. The liposome sample used in that investigation was prepared identically to those used here. The isotonic values $\langle R\rangle_e = 38 \pm 7$ nm and $\langle V\rangle_e = 2.7 \pm 0.6$ μl/mg for SOPC, inferred in this study, are in excellent agreement with an independent entrapped Mn^{2+} measurement, performed under similar conditions, that yielded $\langle V\rangle_e = 2.4 \pm 0.3$ μℓ/mg (Huster et al. 1997). In addition, we have derived such entrapped volume parameters for other liposome lipid compositions and solvent conditions (data not shown). We find that, under identical filtering and extrusion procedures in their isotonic media, these vesicle populations all have similar morphological parameters, e.g. the elongation $p^{-1} = 3.7 \pm 0.6$ and the radius $\langle R\rangle_e = 38 \pm 7$ nm. This is consistent with the above-discussed liposome formation mechanism by extrusion where bilayer properties only have secondary effects (see also Hunter and Frisken 1998).

Assumptions about liposome morphology: model limitations

The results based on Eq. (19) will represent long axis to short axis ratios only when vesicle shapes are close to that of prolate ellipsoids. Otherwise, the elongation parameter derived from Eq. (19) no longer will have a simple meaning, although it still should be indicative of vesicle elongation. Indeed, modeling vesicles as prolate ellipsoids is a simplification (see Introduction). While an ellipsoidal vesicle may correspond approximately to energy minimum under certain conditions, alternative membrane energetic models have been advanced recently (Seifert 1996; Seifert and Lipowsky 1996). In any case, vesicle shape fluctuations can induce further complications given the smallness of the bending energy change estimated under Eq. (17) (Deuling and Helfrich 1976; Lipowsky 1991; Seifert et al. 1991; Seifert 1996; White et al. 1996). For example, such complications may involve a fluctuation-induced renormalization of the effective Hamiltonian for constraint membranes (Seifert 1996), which can easily alter minimal energy shapes and shape transition phase diagrams. A strong consequence of such renormalization was discovered for interfaces undergoing wetting transitions (Jin and Fisher 1993). The lack of full understanding for vesicle morphology and dynamics under constraints of the sort experienced by extruded vesicles preclude exact treatment of the vesicle populations. In the mean time, the consistency of our data in the regimes I and II suggests that the prolate ellipsoidal model for the extruded vesicles is very good, as long as the internal volume is more than half of the corresponding spherical volume. On the other hand, if the internal volume turns out to be near or less than half of the spherical value, one must consider the possibility of drastically different vesicle shapes, and treat the deduced results with caution.

A related assumption adopted in our analysis of morphological polydispersity is that liposomes have a substantial size range, but unique elongation ratio. As stated in the Introduction, this simplification is at first for the sake of having a minimal number of unknown model parameters. However, it is reasonable in light of the above-discussed extruded vesicle formation mechanism (Clerc and Thomp-

son 1994), where the fluctuation instability (Walstra 1983) suggests a constant length to diameter ratio for all cylindrical fragments from which vesicles are formed [see Eq. (15)]. It is also directly supported by the fact that the measurement values of polydispersity Δ^2 for our extruded vesicles remained constant around 0.14 ± 0.2 during the broad range of osmotic expansion and shrinkage (see Fig. 5B). If there was a significant distribution in vesicle elongation, the measured values of Δ^2 should have decreased with the osmotic expansions as an increasing fraction of the vesicles become fully swollen and spherical. No decrease is observed at all for our extruded samples (Fig. 5B). Also in Fig. 6, the transition between regime I and regime II behavior appears quite abrupt, indicating that most vesicles expand into spheres near the same ambient osmolality.

The choice of analytic form for size distribution, $\wp(R)$, affects vesicle size range parameterizations, but is not crucial to our main morphological results. In the evaluation of the elongation, for example, the choice of $\wp(R)$ enters only via the term $\beta^{M}(\Delta)$ defined in Eq. (6) and approximated in Eqs. (7)–(9). For our typical values of $\Delta^2 = 0.14 \pm 0.2$, the difference in higher-order terms on the right-hand side of Eqs. (7) and (9) is negligible [as one finds, e.g., $\beta^{M=LN}(0.15) = 0.819$ vs. $\beta^{M=SW}(0.15) = 0.835$]. Although the precise characterization of the function $\wp(R)$ is still uncertain (Kolchens et al. 1993; Strawbridge and Hallett 1994; Korgel et al. 1998), the size distribution for extruded vesicles appear to be narrow enough to allow the use of any reasonable and convenient form.

In conclusion, we have presented a simple scheme to evaluate, by combining results of static light scattering and dynamic light scattering, the morphological elongation of the extruded liposomes, their characteristic size range, and experimental parameters relevant to specific applications. Because extruded vesicles in osmotic solutions are both elongated and have a notable size distribution range, one must be sure to include the effect of specific liposome parameters that are truly relevant to the required quantitations. For these purposes we have derived various simplified equations [e.g. Eq. (9) for liposome elongation] in order to encourage their usage in diverse applications. The parameter values and osmotic response behavior demonstrated here for SOPC vesicles are, to a good approximation, applicable to other similarly extruded liposome systems because many morphological characteristics of extruded liposomes are insensitive to bilayer properties.

Appendix: vesicle morphology relations for data analysis

Relations for ideal ellipsoidal vesicles

Consider, first, ideal ellipsoidal vesicle suspensions, i.e., that all vesicles are prolate ellipsoids having a uniform major axis a and a uniform minor axis $b = c = ap$ with $p \le 1$, and having smooth infinitely thin shell walls. In the balance of the text, we often refer to $p^{-1} > 1$ as the vesicle elongation parameter. The *hydrodynamic radius* for such particles is among one of few cases that have been explicitly solved and is given by (Schmitz 1990, p 50)

$$R_h(R_s, p) = \frac{R_s (1-p^2)^{1/2}}{p^{2/3} \ln[(1+(1-p^2)^{1/2})/p]} \equiv f_h(p) R_s \quad \text{(A1)}$$

where $R_S \equiv (3/4\,\pi V)^{1/3} = (a\,b^2)^{1/3}$ is the "equivalent spherical radius". The availability of this analytic expression for R_h is one of the main reasons why ellipsoidal vesicle models are practically convenient. Similarly, the radius of gyration for such prolate ellipsoids can be straightforwardly computed as

$$R_g(R_s, p) = \frac{R_s}{p^{2/3}} \cdot \left[\frac{1}{4} + \frac{p^2}{2} \left(\frac{p(1-p^2)^{1/2} + 2\arcsin[(1-p^2)^{1/2}]}{p(1-p^2)^{1/2} + \arcsin[(1-p^2)^{1/2}]} \right) \right]^{1/2} \equiv f_g(p) R_s \quad \text{(A2)}$$

White et al. (1996) have previously reported Eq. (A2) and several other relations for ideal ellipsoidal vesicles, using different notation. This expression for R_g depends on the assumption that the scattering intensity is proportional to the square of the membrane area and approximately independent of local vesicle curvatures and optical differences between vesicle interior/exterior media (White et al. 1996).

To link R_S and p to the vesicle entrapped volume – i.e., to the amount of internal volume per unit of lipid mass, which is often used for vesicle characterization – we introduce another geometrical radius parameter, $R_e(R_s, p) \equiv 3\,V/A = 4\,\pi R_s^3 / A(R_s, p)$, where the surface area $A(R_s, p)$ for the vesicles is given as

$$A(R_s, p) = \frac{2\,\pi R_s^2}{p^{1/3}} \left[p + \frac{\arcsin[(1-p^2)^{1/2}]}{(1-p^2)^{1/2}} \right] \equiv 4\,\pi R_s^2 \, f_A(p) \quad \text{(A3)}$$

Hence the quantity R_e is expressed in terms of R_S and p as

$$R_e(R_s, p) \equiv \frac{3V}{A} = \frac{2 R_s p^{1/3} (1-p^2)^{1/2}}{p(1-p^2)^{1/2} + \arcsin[(1-p^2)^{1/2}]} \equiv f_e(p) R_s \quad \text{(A4)}$$

Note that in general R_h, R_g, and R_e differ but, in the limit $p \to 1$ (the case of a sphere), these radii tend to the same value, i.e., $R_h = R_g = R_e = R_s$, and each liposome shape function approaches unity, i.e. $f_h(p \to 1) = f_g(p \to 1) = f_A(p \to 1) = f_e(p \to 1) = 1$.

Finally, we define the quantity, f_V, to be the ratio of liposome volume to that of a spherical vesicle having the same surface area. This parameter provides another useful measure of vesicle non-sphericity. Following Eq. (A3), we have the expression

$$f_V \equiv \frac{(4\,\pi/3)(A/4\,\pi)^{3/2}}{V} = f_A(p)^{3/2} \quad \text{(A5)}$$

with $f_V \to 1$ in the limit $p \to 1$ for spherical vesicles.

Effects of unimodal vesicle size distribution and thin-wall corrections

Equations (A1)–(A5) pertain to vesicles of exactly uniform size and infinitely thin shell. To apply the same strategy to characterize the extruded vesicles, we must first consider modifications resulting from a narrow *distribution* of vesicle sizes and/or shapes, in accord with the small but nonzero values of Δ^2 determined from dynamic light scattering measurements. Such measured dispersion affects the interpretation of the experimentally determined values $\langle R\rangle_g$, $\langle R\rangle_h$, and many other parameters relevant to specific applications. The intensity-weighted quantities $\langle R\rangle_g$ and $\langle R\rangle_h$ depend *in unlike ways* on the population distribution of various species of particles. Assuming, here, that the particles in our lipid suspensions differ in size R_s *but not in the axial ratio p*, we may express $\langle R\rangle_g$ as

$$\langle R\rangle_g \equiv \left\langle R_g^2\right\rangle_z^{1/2} = \left[\frac{\int [R_g(R_s,p)]^2\,[A(R_s,p)]^2\,\mathfrak{p}(R_s)\,dR_s}{\int [A(R_s,p)]^2\,\mathfrak{p}(R_s)\,dR_s}\right]^{1/2}$$
$$= f_g(p)\sqrt{\frac{\langle R_s^6\rangle}{\langle R_s^4\rangle}} \qquad \text{(A6)}$$

where $\mathfrak{p}(R_S)\,dR_S$ is the number fraction of particles in the suspension having an equivalent radius lying between R_S and R_S+dR_S, and the subscript-free notation $\langle R_S^n\rangle \equiv \int R_S^n\,\mathfrak{p}(R_S)\,dR_S$ represents the simple number-weighted average over the vesicle population. Note that, in the above, the surface area $A(R_S, p)$ [see Eq. (A3)] is proportional approximately to the number of lipid molecules in a thin-shell particle, so $[A(R_S, p)]^2$ is proportional to the intensity of light scattered by such a particle. Similarly, $\langle R\rangle_h$ can be expressed as

$$\langle R\rangle_h \equiv \frac{1}{\left\langle R_h^{-1}\right\rangle_z} = \left[\frac{\int [A(R_s,p)]^2\,\mathfrak{p}(R_s)\,dR_s}{\int [R_h(R_s,p)]^{-1}\,[A(R_s,p)]^2\,\mathfrak{p}(R_s)\,dR_s}\right]$$
$$= f_h(p)\,\frac{\langle R_s^4\rangle}{\langle R_s^3\rangle} \qquad \text{(A7)}$$

where $f_h(p)$ and $f_g(p)$ are the geometrical factors defined in Eqs. (A1) and (A2). It is clear from Eqs. (A6) and (A7) that R_g and R_h have different dependences on the statistical moments of R_s because they are different measures of "average" radius when particle size is not strictly uniform.

For our extruded vesicles, dynamic light scattering measurements suggest relatively narrow, unimodal distributions with small polydispersity, Δ^2 [see Eq. (4) of the text]. In the same way that the expression given in Eq. (A7) for $\langle R_h^{-1}\rangle_z$ has been derived, one can relate $\langle R_h^{-2}\rangle_z$ to the statistical moments $\langle R_S^2\rangle$, $\langle R_S^4\rangle$, etc. Hence, by Eq. (4), we find an alternative expression for Δ^2, as

$$\Delta^2 = \langle R_s^2\rangle\,\langle R_s^4\rangle/[\langle R_s^3\rangle]^2 - 1 \qquad \text{(A8)}$$

Thus the measured value of polydispersity represents a constraint that needs to be satisfied by the actual distribution $\mathfrak{p}(R_S)$, whereas the specific form of $\mathfrak{p}(R_S)$ is not uniquely determined a priori. Although determination of the details of $\mathfrak{p}(R_S)$ appears problematic, many relevant liposome parameters may turn out to be rather insensitive to reasonable choices of such analytic form, so long as the distribution is relatively narrow.

To assess the effect of $\mathfrak{p}(R_S)$ on our morphological analysis, we focus on two illustrative distributions for scattered intensity $\mathfrak{p}_I(R)$, the latter being the fraction of the intensity scattered from particles between size R and $R+dR$ and known to have a relatively narrow and unimodal profile. We assume, as the first example, that $\mathfrak{p}_I(R_S)$ can be approximated by a log-normal distribution

$$\mathfrak{p}_I^{LN}(R_s) = \frac{\exp(-\delta^2/2)}{\sqrt{2\pi}\,R_0\,\delta}\,\exp\left\{-(\ln(R_s)-\ln R_0)^2/(2\delta^2)\right\} \qquad \text{(A9)}$$

and, as the second example, by a square-wave distribution

$$\mathfrak{p}_I^{SW}(R_s) = \left(\frac{1}{\tilde R_0\,\tilde\delta}\right)\left[\Phi(R_s-\tilde R_0) - \Phi(R_s-\tilde R_0(1+\tilde\delta))\right] \qquad \text{(A10)}$$

where $\{\Phi(x\ge 0)=1,\ \Phi(x<0)=0\}$ is the usual step function and the pre-factors assure the normalization, $\int \mathfrak{p}_I(R)\,dR = 1$. Note that $\mathfrak{p}_I(R)$ is related to the vesicle number distribution $\mathfrak{p}(R)$ according to $\mathfrak{p}_I(R) \propto R^4\,\mathfrak{p}(R)$. As seen in Fig. 4, a unique feature of the log-normal distribution is that the corresponding particle number distribution $\mathfrak{p}^{LN}(R)$ is also log-normal, having the same δ but the center value shifted to $R_{0N} = R_0\exp(-4\,\delta^2)$. However, the particle number distribution $\mathfrak{p}^{SW}(R)$ for the square-wave form is a truncated power-law with abrupt cutoffs.

These distributions can be used to evaluate the moments, $\langle R_S^2\rangle$, $\langle R_S^3\rangle$, etc., which appear in Eq. (A8), leading to expressions that relate the distribution parameters δ and $\tilde\delta$ to the polydispersity Δ^2. For the log-normal distribution, we find

$$\delta^2 = \ln(1+\Delta^2) = \Delta^2 - \frac{1}{2}\Delta^4 + \frac{1}{3}\Delta^6 + o(\Delta^8) \qquad \text{(A11)}$$

and correspondingly for the square-wave distribution

$$\tilde\delta^2 = 12\,\Delta^2 + (12\,\Delta^2)^{3/2} + O(\Delta^4) \cong 12\,\Delta^2 + (15.5\,\Delta^2)^2 \qquad \text{(A12)}$$

The latter is obtained from the exact relation $\Delta^2 = \tilde\delta^2[(1+\tilde\delta)(\ln(1+\tilde\delta))^2] - 1$, using an equation discovery program (TableCurve 2D, Jandel Scientific software). These allow us to express the moments $\langle R_S^2\rangle$, $\langle R_S^3\rangle$, … in terms of the unknown distribution center value R_0 or $\tilde R_0$ and the measured parameter Δ as

$$\left\langle R_s^n\right\rangle \equiv \alpha_n^{LN}(\Delta)\,R_0^n = R_0^n\,(1+\Delta^2)^{n(n-6)/2}$$
$$= R_{0N}^n(1+\Delta^2)^{n(n+2)/2} \qquad \text{(A13)}$$

and,

$$\left\langle R_s^n\right\rangle \equiv \alpha_n^{SW}(\Delta)\,\tilde R_0^n = \tilde R_0^n\,\frac{3}{(1+\tilde\delta(\Delta))^{-3}-1}$$
$$\cdot\left[(1+\tilde\delta(\Delta))^{n-3}-1\right]/[n-3] \qquad \text{(A14)}$$

where, as $n \to 3$, $[(1+\tilde{\delta})^{n-3}-1]/(n-3) \to \ln(1+\tilde{\delta})$ is understood. The expressions reveal that the effect of a narrow dispersion in vesicle sizes is to cause the factors $\alpha_n^{\mathrm{LN}}(\Delta)$ or $\alpha_n^{\mathrm{SW}}(\Delta)$ to increase as the power n increases in ways depending on the analytic form of the assumed size distribution. The use of Eqs. (A13), (A14), etc., in our analysis will show that the main results are fairly insensitive to particular distribution forms.

Returning to consideration of the measured quantities $\langle R\rangle_{\mathrm{h}}$ and $\langle R\rangle_{\mathrm{g}}$, we note that the finite thickness of the vesicle walls necessitates some additional consideration. Because $\langle R\rangle_{\mathrm{h}}$ is related to the diffusive motions of the vesicles, it is a measure of a dimension linked to the outer surfaces of the vesicles. However, $\langle R\rangle_{\mathrm{g}}$, which is determined from the total scattering intensity, should roughly correspond to the middle plane of the bilayer, whereas the entrapped volume parameter depends on the inner dimensions of the vesicle walls. Because the wall thickness ℓ of a typical vesicle is approximately 4 nm, we can arbitrarily choose the outer surface as a reference, and increase the measured values of $\langle R\rangle_{\mathrm{g}}$ and $\langle R\rangle_{\mathrm{e}}$ by $\ell/2$ and ℓ, respectively, to obtain comparative expressions for R_0. Since our extruded vesicle samples have a typical measured radius of 50 nm, these thin-wall corrections are of about 4% and 8%, respectively, and the slight error in the value of ℓ (e.g., that due to the vesicle bilayer structural changes under small osmotic stress and a hydation layer of about 0.3 nm) is not significant.

Acknowledgement The light scattering measurements were carried out in the Laboratory of Molecular Biology, NIDDK, NIH.

References

Allen TM, Austin GA, Chonn A, Lin L, Lee KC (1991) Uptake of liposomes by cultured mouse bone marrow. Biochim Biophys Acta 1061: 56–64

Aragon SR, Pecora R (1976) Theory of dynamic light scattering from polydisperse systems. J Chem Phys 64: 2395–2404

Arshady R (1993) Microcapsules for food. J Microencapsulation 10: 413–435

Choquet CG, Patel GB, Beveridge TJ, Sprott GD (1994) Stability of pressure-extruded liposomes. Appl Microbiol Biotechnol 42: 375–384

Clerc SG, Thompson TE (1994) A possible mechanism for vesicle formation by extrusion. Biophys J 64: 475–477

Dahneke BE (ed) (1983) Measurement of suspended particles by quasi-elastic light scattering. Wiley, New York

Deuling HJ, Helfrich W (1976) The curvature elasticity of fluid membranes: a catalogue of vesicle shapes. J Phys (Paris) 37: 1335–1345

Ertel A, Marangoni AG, Marsh J, Hallett FR, Wood JM (1993) Mechanical properties of vesicles I: coordinated analyses. Biophys J 64: 426–434

Farge E, Devaux PF (1992) Shape changes of giant liposomes induced by an asymmetric transmembrane distribution of phospholipids. Biophys J 61: 347–357

Fresta M, Puglisi G (1997) Corticosteroid dermal delivery with skin-lipid liposomes. J Controlled Release 44: 141–151

Fresta M, Wehrli E, Puglisi G (1995) Neutrase entrapment in stable multilamellar and large unilamellar. J Microencapsulation 12: 307–325

Hallett FR, Marsh J, Nickel BG, Wood JM (1993) Mechanical properties of vesicles II. A model for osmotic swelling and lysis. Biophys J 64: 435–442

Hallett FR, Watton J, Krygsman P (1991) Vesicle sizing: number distributions by dynamic light scattering. Biophys J 59: 357–362

Hill KJ, Kaszuba M, Creeth JE, Jones MN (1997) Reactive liposomes encapsulating a glucose oxidase-peroxidase system with antibacterial activity. Biochim Biophys Acta 1326: 37–46

Hontoria F, Crowe JH, Crowe LM, Amat F (1994) Potential use of liposomes in larviculture as a delivery system through Artemia nauplii. Aquaculture 127: 255–264

Hope MJ, Bally MB, Webb G, Cullis PR (1985) Production of large unilamellar vesicles by a rapid extrusion procedure. Characterization of size distribution, trapped volume and ability to maintain a membrane potential. Biochim Biophys Acta 812: 55–65

Hunter DG, Frisken BJ (1998) Effect of extrusion pressure and lipid properties on the size and polydispersity of lipid vesicles. Biophys J 74: 2996–3002

Huster D, Jin AJ, Arnold K, Gawrisch K (1997) Water permeability of polyunsaturated lipid membranes measured by ^{17}O NMR. Biophys J 73: 855–864

Jin AJ, Fisher ME (1993) Stiffness instability in short-range critical wetting. Phys Rev B 48: 2642–2658

Kas J, Sackmann E (1991) Shape transitions and shape stability of giant phospholipid vesicles in pure water induced by area-to-volume changes. Biophys J 60: 825–844

Koenig BK, Strey HH, Gawrisch K (1997) Membrane lateral compressibility determined by NMR and x-ray diffraction: effect of acyl chain polyunsaturation. Biophys J 97: 1954–1966

Kolchens S, Ramaswami N, Birgenheier J, Nett L, Obrien DF (1993) Quasi-elastic light scattering determination of the size distribution of extruded vesicles. Chem Phys Lipids 65: 1–10

Komatsu H, Guy PT, Rowe ES (1993) Effect of unilamellar vesicle size on ethanol-induced interdigitation in dipalmitoylphosphatidylcholine. Chem Phys Lipids 65: 11–21

Korgel BA, van Zanten JH, Monbouquette HG (1998) Vesicle size distributions measured by flow field-flow fractionation coupled with multiangle light scattering. Biophys J 74: 3264–3272

Lasic DD, Barenholz Y (eds) (1996) Handbook of nonmedical applications of liposomes: theorey and basic scienes. CRC Press, New York

Lentz BR, Mcintyre GF, Parks DJ, Yates JC, Massenburg D (1992) Bilayer curvature and certain amphipaths promote polyethylene glycol-induced fusion of dipalmitoylphosphatidylcholine unilamellar vesicles. Biochemistry 31: 2643–2653

Lesieur S, Grabielle Madelmont C, Paternostre MT, Ollivon M (1991) Size analysis and stability study of lipid vesicles by. Anal Biochem 192: 334–343

Lipowsky R (1991) The conformation of membranes. Nature 349: 475–481

Liu D, Mori A, Huang L (1991) Large liposomes containing ganglioside gm-1 accumulate effectively in spleen. Biochim Biophys Acta 1066: 159–165

Mayer LD, Hope MJ, Cullis PR (1986) Vesicle of various sizes produced by a rapid extrusion procedure. Biochem Biophys Acta 858: 161–168

Monshipouri M, Rudolph AS (1995) Liposome-encapsulated alginate: controlled hydrogen particle formation and release. J Microencapsulation 12: 117–127

Mui BLS, Cullis PR, Evans EA, Madden TD (1993) Osmotic properties of large unilamellar vesicles prepared by extrusion. Biophys J 64: 443–453

Needham D, Nunn RS (1990) Elastic deformation and failure of lipid bilayer membranes containing cholesterol. Biophys J 58: 997–1009

Nossal R, Weiss GH, Nandi PK, Lippoldt RE, Edelhoch H (1983) Size and mass distributions of clathrin-coated vesicles from bovine brain. Arch Biochem Biophys 226: 593–603

Ostro MJ (ed) (1987) Liposomes: from biophysics to therapeutics. Dekker, New York

Phillippot JR, Schuber F (eds) (1995) Liposomes as tools in basic research and industry. CRC Press, Ann Arbor

Rock PA (1969) Chemical thermodynamics: Principles and applications. Macmillan, London

Schmitz KS (1990) An introduction to dynamic light scattering by macromolecules. Academic Press, Boston

Seifert U (1996) Morphology and dynamics of vesicles. Curr Opin Coll Int Sci 1:350–357
Seifert U, Lipowsky R (1996) Shapes of fluid. In: Lasic DD, Barenholz Y (eds) Handbook of nonmedical applications of liposomes: theory and basic sciences. CRC Press, New York, pp 43–68
Seifert U, Berndl K, Lipowsky R (1991) Shape transformations of vesicles: phase diagram for spontaneous-curvature and bilayer-coupling models. Phys Rev A 44:1182–1201
Selser JC, Yeh Y, Baskin RJ (1976) A light scattering characterization of membrane vesicles. Biophys J 16:337–356
Strawbridge KB, Hallett FR (1994) Size distributions obtained from the inversion of I(Q) using integrated light scattering spectroscopy. Macromolecules 27:2283–2290
Tabak A, Hoffer E, Taitelman U (1994) Evaluation of a liposome system for the delivery of desferrioxamine to lungs in rats. J Pharm Pharmacol 46:789–796
Templeton NS, Lasic DD, Frederik PM, Strey HH, Roberts DD (1997) Improved DNA: liposome complexes for increased systemic delivery and gene expression. Nat Biotechnol 15:647–652
Walker SA, Kennedy MT, Zasadzinski JA (1997) Encapsulation of bilayer vesicles by self-assembly. Nature 387:61–64
Walstra P (1983) Basic theory. In: Becker P (ed) Encyclopedia of emulsion technology, vol 1. Dekker, New York, pp 57–127
White G, Pencer J, Nickel BG, Wood JM, Hallett FR (1996) Optical changes in unilamellar vesicles experiencing osmotic stress. Biophys J 71:2701–2705
Winterhalter M, Lasic DD (1993) Liposome stability and formation: experimental parameters and theories on the size distribution. Chem Phys Lipids 64:35–43
Woodle MC, Storm G (eds) (1998) Long circulating liposomes: old drugs, new therapeutics. Springer, Berlin Heidelberg New York